Effects of Al particles and thin layer on thermal expansion and conductivity of Al–$Y_2Mo_3O_{12}$ cermets*

Xian-Sheng Liu(刘献省)[1], Xiang-Hong Ge(葛向红)[2,3], Er-Jun Liang(梁二军)[2,†], and Wei-Feng Zhang(张伟风)[1,‡]

[1] *Henan Key Laboratory of Photovoltaic Materials and Laboratory of Low Dimensional Materials Science, School of Physics and Electronics, Henan University, Kaifeng* 475004, *China*

[2] *School of Physical Science & Engineering and Key Laboratory of Materials Physics of Ministry of Education of China, Zhengzhou University, Zhengzhou* 450051, *China*

[3] *Zhongyuan University of Technology, Zhengzhou* 450007, *China*

(Received 8 May 2017; revised manuscript received 13 July 2017; published online 29 September 2017)

Low thermal expansion composites are difficult to obtain by using Al with larger positive thermal expansion coefficient (TEC) and the materials with smaller negative TECs. In this investigation, $Y_2Mo_3O_{12}$ with larger negative TEC is used to combine with Al to obtain a low thermal expansion composite with high conductivity. The TEC of Al is reduced by 19% for a ratio Al:$Y_2Mo_3O_{12}$ of 0.3118. When the mass ratio of Al:$Y_2Mo_3O_{12}$ increases to 2.0000, the conductivity of the composite increases so much that a transformation from capacitance to pure resistance appears. The results suggest that $Y_2Mo_3O_{12}$ plays a dominant role in the composite for low content of Al (presenting isolate particles), while the content of Al increases enough to contact each other, the composite presents mainly the property of Al. For the effect of high content Al, it is considered that Al is squeezed out of the cermets during the uniaxial pressure process to form a thin layer on the surface.

Keywords: negative thermal expansion, low thermal expansion, conductivity, composite

PACS: 81.05.Mh, 65.40.De, 72.10.Fk **DOI:** 10.1088/1674-1056/26/11/118101

1. Introduction

The mechanisms and applications of negative thermal expansion (NTE) materials attract more and more investigations because of their special roles in reducing thermal expansion coefficients of composites.[1–10] Owing to some disadvantages, such as metastable structure, smaller NTE coefficient, poor mechanics, low electrical conductivity, much higher phase transition temperature than room temperature, hygroscopicity, etc., the extensive applications of NTE materials are still the challenges.[4–13] Adopting metal (such as Al, Cu) to combine with NTE materials is meaningful to improve the electrical and mechanical properties. Therefore, there are some reports about Al–ZrW_2O_8,[14] Cu–ZrW_2O_8,[15–19] Cu–$Sc_2W_3O_{12}$,[20] Al–ZrV_2O_7,[21] Al–$Zr_2(WO_4)(PO_4)_2$,[22] Al–$ZrMgMo_3O_{12}$.[23] However, due to the metastable structure, the decomposition of ZrW_2O_8 is easy to appear when combining ZrW_2O_8 with metal Al/Cu. The ZrV_2O_7 presents abrupt thermal expansion before the phase transition from a $3\times3\times3$ cubic superstructure to a normal parent cubic structure at 375 K, and only the latter structure presents NTE,[24,25] especially, the reaction products of $AlVO_3$, $AlVO_4$ and cubic $Zr_{1-x}Al_xV_2O_7$ from the reactions between Al and ZrV_2O_7 affect the NTE behavior.[21] The $Sc_2W_3O_{12}$ contains a rare metal element of Sc, which largely restricts the application of Cu–$Sc_2W_3O_{12}$. It is difficult to obtain low thermal expansion compositions by using $Zr_2(WO_4)(PO_4)_2$ and $ZrMgMo_3O_{12}$ with much lower NTE coefficients of than that of Al.[20,22,23] Consequently, it is meaningful to adopt the NTE material with stable structure, larger NTE coefficient, but without rare element to combine with metal materials.

For the $A_2M_3O_{12}$ (A: trivalent anion, M: W or Mo) family, with stable structures, only some of them with larger A^{3+} ion radii, such as Y^{3+}, Yb^{3+}, Er^{3+}, etc., have larger NTE coefficients. The others with smaller ionic radii of A^{3+}, such as Fe^{3+}, Al^{3+}, Cr^{3+}, In^{3+}, etc., have lower NTE coefficients. Therefore, stable NTE materials with more negative coefficients of $A_2M_3O_{12}$ could be suited to obtain low thermal expansion by combining with metal Al. However, so far, there are few reports on adopting metal materials to combine with $A_2M_3O_{12}$ with larger A^{3+} ion radii such as Y^{3+}, Yb^{3+}, Er^{3+}, etc. (the reason relates to their heavy hygroscopicities).[20] Whether the influence of heavy hygroscopicity on the properties of Al–$A_2M_3O_{12}$ can be reduced by the introduction of Al can only be confirmed experimentally. Therefore, it is meaningful to study the combination of Al and $Y_2Mo_3O_{12}$ with larger negative coefficient.

*Project supported by the National Natural Science Foundation of China (Grant Nos. 10974183 and 11104252), the Doctoral Fund of the Ministry of Education of China (Grant No. 20114101110003), the Fund for Science & Technology Innovation Team of Zhengzhou, China (Grant No. 112PCXTD337), the Industrial Science and Technology Research Projects of Kaifeng, Henan Province, China (Grant No. 1501049), and the Key Research Projects of Henan Higher Education Institutions, China (Grant No. 18A140014).

†Corresponding author. E-mail: ejliang@zzu.edu.cn

‡Corresponding author. E-mail: wfzhang@henu.edu.cn

© 2017 Chinese Physical Society and IOP Publishing Ltd

In the paper, $Y_2Mo_3O_{12}$ is prepared by the solid state method and combined with metal Al powders to obtain low thermal expansion Al–$Y_2Mo_3O_{12}$ cermet. The hygroscopicity, the thermal expansion property and conductivity of Al–$Y_2Mo_3O_{12}$ are investigated. The thermal expansion of Al is reduced by 19% for the ratio Al:$Y_2Mo_3O_{12}$ of 0.3118 and the hygroscopicity of $Y_2Mo_3O_{12}$ also decreases notably. The transformation of electrical property from capacitance to pure resistance with the mass ratio of Al:$Y_2Mo_3O_{12}$ increasing to 2.0000 suggests the notable enhancement of conductivity. For high content of Al, it is considered that much Al is squeezed out of the cermet Al–$Y_2Mo_3O_{12}$ during the uniaxial pressure process.

2. Experiment

$Y_2Mo_3O_{12}$ was prepared with solid state method using analytical grade Y_2O_3 and MoO_3 as raw materials (molar ratio of Y:Mo = 2:3). The raw materials were weighted and ground for 2 h followed by sintering at 1073 K for 5 h to obtain white powders of $Y_2Mo_3O_{12}$. For the preparation of Al–$Y_2Mo_3O_{12}$ composites, the prepared $Y_2Mo_3O_{12}$ powders and commercial Al powders (through 200 mesh sieve) were mixed with different Al:$Y_2Mo_3O_{12}$ mass ratios and ground for 2 h. The dried powder compositions were cold-pressed into cylinders (10 mm in diameter and 15 mm in length for linear thermal expansion measurements) or pellets (10 mm in diameter and 2 mm in thickness for electrical property measurements) by uniaxial pressure at 300 MPa. Then the specimens were sintered at 953 K for 1 h to obtain Al–$Y_2Mo_3O_{12}$ cermets.

The x-ray diffraction (XRD) measurements were carried out with an x-ray diffractometer (Model X'Pert PRO) to identify the crystalline phase. The microstructure and chemical compositions of the samples were observed with a field emission scanning electron microscope (FE-SEM, Model JSM-6700F) combined with energy dispersive spectrometry (EDS, ISIS400). The linear thermal expansion coefficient was measured with a dilatometer (LINSEIS DIL L76). The impedance spectra were recorded on the Precision Impedance Analyzer (Agilent 4294A).

3. Results and discussion

3.1. Crystal structure

Figure 1 shows the XRD patterns of Al–$Y_2Mo_3O_{12}$ cermets. It is found that the diffraction peaks of $Y_2Mo_3O_{12}$ are weak, which are related to its hygroscopicity.[11,26] Due to the interaction between H_2O and Y–O–Mo in $Y_2Mo_3O_{12}$, the symmetry of $Y_2Mo_3O_{12}$ is reduced and so is the symmetry of crystallinity. With increasing the content of Al in the cermet of Al–$Y_2Mo_3O_{12}$, some peaks corresponding to Al (ICDD-PDF No. 01-085-1327) become higher in intensity and the peaks belonging to $Y_2Mo_3O_{12}$ turn much weaker. Except for the peaks corresponding to Al and $Y_2Mo_3O_{12}$, no more unknown peaks are observed, indicating that there are no other new decompositions from $Y_2Mo_3O_{12}$ and no reactions between $Y_2Mo_3O_{12}$ and Al in their sintering process either.

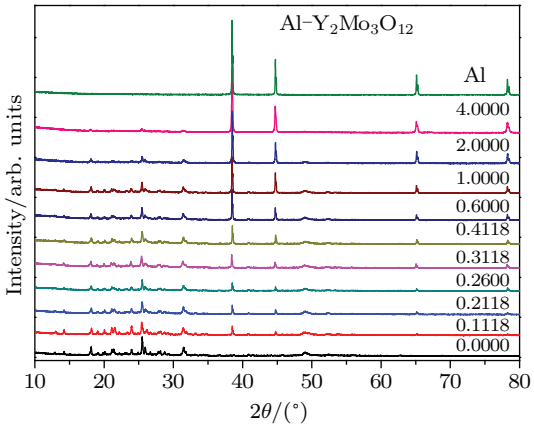


Fig. 1. (color online) XRD patterns of Al–$Y_2Mo_3O_{12}$ cermets with different mass ratios of Al:$Y_2Mo_3O_{12}$.

3.2. Low thermal expansion

Figure 2 shows relative linear length changes of Al–$Y_2Mo_3O_{12}$ cermets with increasing temperature. The pure ceramic $Y_2Mo_3O_{12}$ presents obvious shrinkage in a temperature range of 353–408 K, which is corresponding to the release of crystal water with weak interaction with a lattice of $Y_2Mo_3O_{12}$.[11] However, an abrupt expansion in a temperature range of 408–453 K is observed and ascribed to the release of crystal water with a strong interaction with a lattice of $Y_2Mo_3O_{12}$.[11] The crystal water is adsorbed on the surface of $Y_2Mo_3O_{12}$ with weak interaction, i.e., the crystal water exists among the molecule groups of $Y_2Mo_3O_{12}$. The distance between $Y_2Mo_3O_{12}$ increases due to the crystal water among the molecule groups of $Y_2Mo_3O_{12}$. Therefore, the release of crystal water with weak interaction induces the smaller distance and then the shrinkage of $Y_2Mo_3O_{12}$. For the crystal water among the molecules of $Y_2Mo_3O_{12}$ with strong interaction, the forming bonds (O···H–O···A) between hydroxy group OH^- in crystal water and O/A^{3+} in A–O–M linkages restrict the transverse vibration of the bridge oxygen atom in A–O–M linkage, which is responsible for NTE. The crystal water among the molecules of $Y_2Mo_3O_{12}$ with strong interaction drags different molecules of $Y_2Mo_3O_{12}$ more closely and then $Y_2Mo_3O_{12}$ crystals contract each other. Therefore, the release of crystal water with strong interaction induces an abrupt expansion of $Y_2Mo_3O_{12}$.

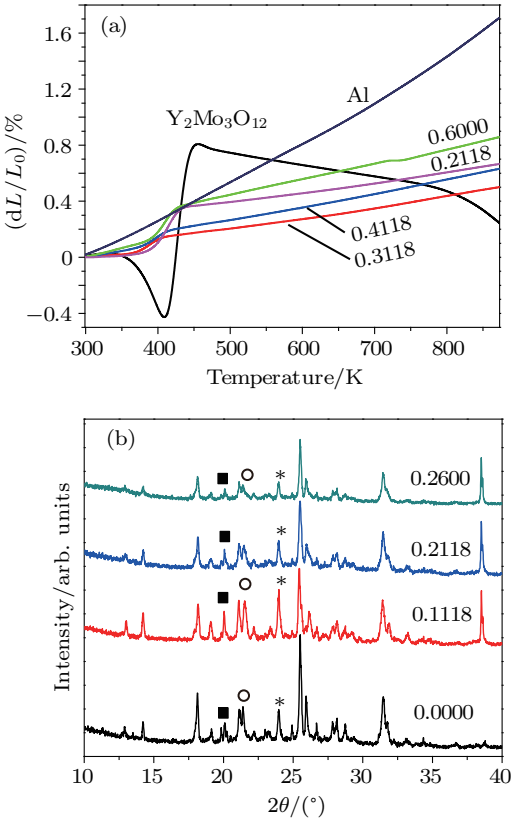


Fig. 2. (color online) (a) Relative linear length changes of Al–$Y_2Mo_3O_{12}$ cermets with increasing temperature. (b) Amplified XRD patterns of Al–$Y_2Mo_3O_{12}$ with molar ratios of 0.0000, 0.1118, 0.2118, 0.2600.

After the complete release of crystal water, the ceramic $Y_2Mo_3O_{12}$ shows obviously the NTE property. With increasing the mass ratio of Al:$Y_2Mo_3O_{12}$, the shrinkage and abrupt thermal expansion corresponding to temperature ranges of 353–408 K and 408–453 K are weakened and their temperature ranges also shift to lower temperature ranges. Especially, for the samples with mass ratios of 0.3118 and 0.4118 as their temperature increases from 410 K to 873 K, the coefficients of thermal expansion reach about 5.69×10^{-6} K^{-1} and 8.13×10^{-6} K^{-1}, respectively. The coefficient of thermal expansion of Al, as temperature increases from 300 K to 873 K, is 29.84×10^{-6} K^{-1}, which is about 5.2 and 3.7 times those of the samples with mass ratios of 0.3118 and 0.4118, respectively. The result shows that the thermal expansion of Al is much reduced by combining with $Y_2Mo_3O_{12}$.

In order to explore the mechanism for reducing thermal expansion of Al–$Y_2Mo_3O_{12}$, we re-investigate the XRD patterns by amplifying local region (10°–40°). Figure 2(b) shows the amplified XRD patterns (Fig. 1) of Al–$Y_2Mo_3O_{12}$ with molar ratios of 0.0000, 0.1118, 0.2118, and 0.2600. It is found that the diffraction peaks are at about 20°, 21°, 24°, indicating that the values marked with signs of ■, ◯ and ∗ change notably in relative intensity and peak splitting: the two diffraction peaks at about 20° turn into one main peak, the diffraction peaks at about 21° split much completely, and the relative intensity of the diffraction peak at about 24° increases greatly. The results suggest that the crystal of $Y_2Mo_3O_{12}$ doped with Al displays mixture polymorphs of *Pba*2 and *Pbcn*.[26] The crystal structure change could result from a few Al atoms entering into the lattice of $Y_2Mo_3O_{12}$, repelling the water molecules and releasing the translation vibrations of bridge oxygen atoms for the NTE property. On the other hand, other effects of hygroscopicity on the XRD patterns of $Y_2Mo_3O_{12}$ are shown, such as, the additional peak at about 13.5° and peak splitting at about 20°.

Figure 3 shows a schematic diagram of the effect of the introduction of Al on the crystal water in $Y_2Mo_3O_{12}$. Before the introduction of Al, crystal water interacts with Y–O–Mo in $Y_2Mo_3O_{12}$, which affects the transverse motion of bridge oxygen in Y–O–Mo and also the thermal expansion.[7,11] After the introduction of Al, the contribution of electrons from Al to O in Y–O–Mo reduces the magnitude and influence of crystal water,so that the crystal water with strong interaction with a lattice of $Y_2Mo_3O_{12}$ is completely released by increasing the content of Al. Consequently, $Y_2Mo_3O_{12}$ regains its NTE property affected by crystal water and Al–$Y_2Mo_3O_{12}$ cermets with larger mass ratios present lower thermal expansions than pure Al.

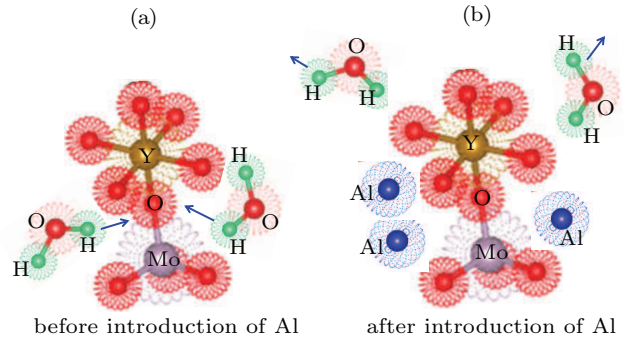


Fig. 3. (color online) Schematic diagram of the effect of introduction of Al on the crystal water in $Y_2Mo_3O_{12}$. (a) Before introduction of Al and (b) after introduction of Al.

3.3. Enhanced conductivity

In order to make clear the effect of Al on ceramic $Y_2Mo_3O_{12}$, we investigate the impedance properties of $Y_2Mo_3O_{12}$ and Al–$Y_2Mo_3O_{12}$ cermets. The impedance spectra of $Y_2Mo_3O_{12}$ and Al–$Y_2Mo_3O_{12}$ cermets are shown in Fig. 4. It is found that the pure $Y_2Mo_3O_{12}$ presents the capacitance property of impedance, which decreases with frequency increasing. As the mass ratio of Al:$Y_2Mo_3O_{12}$ increases, the impedance curves present first an increase trend (from 0.1118 to 0.3118) and then a decrease trend (from 0.4118 to 1.0000). Especially from 2.0000 to 4.0000, the impedance spectra transform to linear lines with pure resistance property, whose impedances remain the same even when increasing the frequency. The results of impedance spectra could be analyzed as follows.

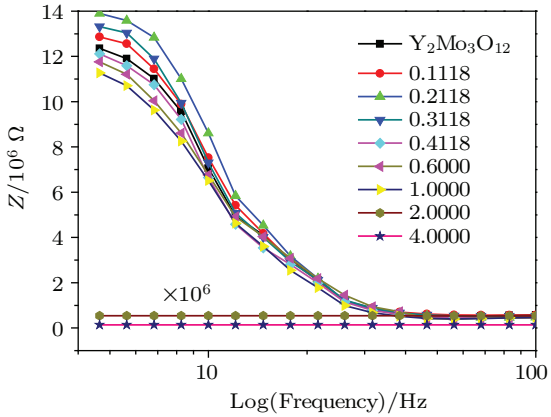


Fig. 4. (color online) Impedance spectra of $Y_2Mo_3O_{12}$ and Al–$Y_2Mo_3O_{12}$ cermets.

For the lower mass ratios $\leq$0.3118, crystal water decreases with the Al content increasing. It is reasonable that the electrons from introduced Al contribute to the conductivity, however, in ceramic $Y_2Mo_3O_{12}$ with segregated Al grains, electrons are difficult to transfer far away. For the larger mass ratios $>$ 0.3118 but $\leq$1.0000, more Al elements in Al–$Y_2Mo_3O_{12}$ cermets contact each other and act as metal plates to form serial connected capacitors, thereby increasing the transportation of electrons and reducing the impedance. Especially, for much larger mass ratios $\geq$ 2.0000, the content of metal Al increases enough for contacting each other to form channels for electrons. Therefore, the impedance decreases abruptly and the Al–$Y_2Mo_3O_{12}$ cermets present pure resistance property. The results suggest that the heavy hygroscopicity of NTE ceramic could be reduced remarkably by combining with metal Al and the formed cermets with high conductivity and low thermal expansion might find applications in electrical components. The microstructures of the Al–$Y_2Mo_3O_{12}$ cermets could present some suggestions.

Figure 5 shows the SEM images of Al–$Y_2Mo_3O_{12}$ cermets with mass ratios of 0, 0.1118, 0.2118, 0.6000, 1.0000, and 4.0000. For the pure $Y_2Mo_3O_{12}$ ceramic with heavy hygroscopicity, there are many pores among the grains with various shapes. With increasing the mass ratio of Al:$Y_2Mo_3O_{12}$, the pores among grains decrease remarkably and nearly spherical grains increase much more. The decreasing of the pores among grains is considered to relate to the filling of melt Al in the interspaces among the $Y_2Mo_3O_{12}$ grains.[22,23] For a mass ratio of 0.2118, the pores between grains decrease obviously but still exist. When the mass ratio reaches 0.6000, there are few pores to be observed. Comparing the SEM images of Al–$Zr_2(WO_4)(PO_4)_2$ and Al–$ZrMgMo_3O_{12}$, there are less pores for Al–$Y_2Mo_3O_{12}$ cermets with a similar content of Al,[22,23] which could relate to the low sintering temperature for $Y_2Mo_3O_{12}$. The increase of nearly spherical grains should relate to the decreasing of crystal water of $Y_2Mo_3O_{12}$. As for the sample with a mass ratio of 4.0000, the metal characteristic is obvious due to the covering effect of the Al thin layer on the surface of Al–$Y_2Mo_3O_{12}$ cermets, which results in fixed impedances even when increasing the frequency.

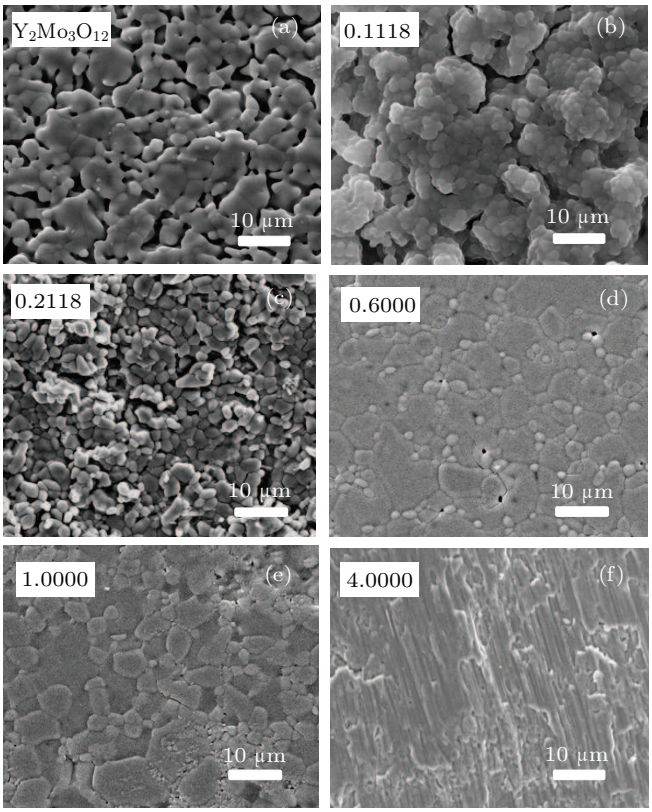


Fig. 5. SEM images of Al–$Y_2Mo_3O_{12}$ cermets with mass ratios of (a) 0, (b) 0.1118, (c) 0.2118, (d) 0.6000, (e) 1.0000, and (f) 4.0000.

4. Conclusions

Al–$Y_2Mo_3O_{12}$ cermets are prepared, and low thermal expansion and enhanced conductivity are obtained. The larger NTE coefficient of $Y_2Mo_3O_{12}$ results in low thermal expansion of Al–$Y_2Mo_3O_{12}$. The hygroscopicity of $Y_2Mo_3O_{12}$ is reduced obviously by introducing the Al element. The melting Al among the grains of $Y_2Mo_3O_{12}$ improves the conductivity of the ceramic. Al squeezed out of the cermet Al–$Y_2Mo_3O_{12}$ during the uniaxial pressure process to form a thin layer on the surface of the cermet plays an important role in the thermal expansion and conductivity. The investigation suggests a challenge to tailoring the thermal expansion coefficient by using larger NTE coefficient $A_2M_3O_{12}$ material and metal Al.

References

[1] Mary T A, Evans J S O, Vogt T and Sleight A W 1996 *Science* **272** 90
[2] Gava V, Martinotto A L and Perottoni C A 2012 *Phys. Rev. Lett.* **109** 195503
[3] Takenaka K, Okamoto Y, Shinoda T, Katayama N and Sakai Y 2017 *Nature Commun.* **8** 14102
[4] Wang L, Wang C, Luo H B and Sun Y 2017 *J. Phys. Chem. C* **121** 333
[5] Marinkovic B A, Ari M, Avillez R R, Rizzo F, Ferreira F F, Miller K J, Johnson M B and White M A 2009 *Chem. Mater.* **21** 2886
[6] Liang E J, Huo H L, Wang J P and Chao M J 2008 *J. Phys. Chem. C* **112** 6577
[7] Li Z Y, Song W B and Liang E J 2011 *J. Phys. Chem. C* **115** 17806

[8] Yuan B H, Yuan H L, Song W B, Liu X S, Cheng Y G, Chao M J and Liang E J 2014 *Chin. Phys. Lett.* **31** 076501
[9] Ge X H, Mao Y C, Li L, Li L P, Yuan N, Cheng Y G, Guo J, Chao M J and Liang E J 2016 *Chin. Phys. Lett.* **33** 046503
[10] Li T, Liu X S, Cheng Y G, Ge X H, Zhang M D, Lian H, Zhang Y, Liang E J and Li Y X 2017 *Chin. Phys. B* **26** 016501
[11] Liu X S, Cheng Y G, Liang E J and Chao M J 2014 *Phys. Chem. Chem. Phys.* **16** 12848
[12] Mittal R and Chaplot S L 2008 *Phys. Rev. B* **78** 174303
[13] Suzukiw T and Omote A 2006 *J. Am. Ceram. Soc.* **89** 691
[14] Matsumoto A, Kobayashi K, Nishio T and Ozaki K 2003 *Mater. Sci. Forum* **426–432** 2279
[15] Verdon C and Dunand D C 1997 *Scripta. Mater.* **36** 1075
[16] Holzer H and Dunand D C 1999 *J. Mater. Res.* **14** 780
[17] Yilmaz S 2002 *Compos. Sci. Technol.* **62** 1835
[18] Yilmaz S and Dunand D C 2004 *Compos. Sci. Technol.* **64** 1895
[19] Liang E J 2010 *Rec. Pat. Mater. Sci.* **3** 106
[20] Liu Q Q, Yang J, Cheng X N, Liang G S and Sun X J 2012 *Ceram. Int.* **38** 541
[21] Yun D Q, Gu Q C and Wang X F 2005 *Acta Mater. Comp. Sci.* **22** 25
[22] Liu X S, Cheng F X, Wang J Q, Song W B, Yuan B H and Liang E J 2013 *J. Alloys Compd.* **553** 1
[23] Xiao X, Zhou W J, Liu X S, Chao M J, Li Y C, Zhang N, Liu Y M, Li Y X, Feng D S and Liang E J 2015 *Ceram. Int.* **41** 2361
[24] Yuan B H, Liu X S, Mao Y C, Wang J Q, Guo J, Cheng Y G, Song W B, Liang E J and Chao M J 2016 *Mater. Chem. Phys.* **170** 162
[25] Yamamura Y, Horikoshi A, Yasuzuka S, Saitoh H and Saito K 2011 *Dalton Trans.* **40** 2242
[26] Gates S D and Lind C 2007 *J. Solid State Chem.* **180** 3510